Diphosphines with Natural Bite Angles near 120° Increase Selectivity for *n*-Aldehyde Formation in Rhodium-Catalyzed Hydroformylation

Charles P. Casey,* Gregory T. Whiteker, Margaret G. Melville, Lori M. Petrovich, James A. Gavney, Jr., and Douglas R. Powell

Contribution from the Department of Chemistry, University of Wisconsin, Madison, Wisconsin 53706. *Received January 14, 1992*

Abstract: The use of 2,2′-bis[(diphenylphosphino)methyl]-1,1′-biphenyl (BISBI, **1**), *trans*-1,2-bis[(diphenylphosphino)-methyl]cyclopropane (T-BDCP, **2**), and other diphosphines with large natural bite angles as ligands in rhodium-catalyzed hydroformylation has been studied. The X-ray crystal structure of (BISBI)Rh(PPh_3)(CO)H·CH_2Cl_2 (**7**·CH_2Cl_2) indicated a trigonal bipyramidal structure with the three phosphorus atoms in the equatorial plane. The P–Rh–P bite angle of the BISBI ligand in **7**·CH_2Cl_2 of 124.8° is much smaller than the 152° P–Fe–P bite angle found in (BISBI)Fe$(CO)_3$ and indicates that the BISBI ligand is rather flexible. NMR studies indicate that rapid exchange ($\Delta G^{\ddagger}$ = 15.5 kcal mol^{-1}) occurs between the coordinated PPh_3 of **7** and free PPh_3. **7** reacted with CO to produce (BISBI)Rh$(CO)_2$H (**9**), which was shown by IR and NMR studies to have a trigonal bipyramidal structure with BISBI in the equatorial plane and hydride in an apical position. The solution structures of the T-BDCP complexes (T-BDCP)Rh(PPh_3)(CO)H (**13**) and (T-BDCP)Rh$(CO)_2$H (**14**) were shown by spectroscopy to be similar to the related BISBI compounds. A correlation between the size of the natural bite angle of chelating diphosphines and the regioselectivity for formation of straight-chain aldehydes in the rhodium-catalyzed hydroformylation of 1-hexene was observed.

Introduction

Hydroformylation is one of the most industrially important homogeneously catalyzed reactions.[1] The very efficient modern rhodium–phosphine catalysts were first developed by Wilkinson[2] and first employed by Union Carbide.[3] Compared to older cobalt hydroformylation catalysts, the rhodium catalysts offer the advantages of enhanced rates, lower operating temperatures and pressures, and higher selectivity for straight-chain aldehydes.

Wilkinson's generally accepted dissociative mechanism for rhodium-catalyzed hydroformylation is shown in Scheme I. The key intermediates in this mechanism are five-coordinate bis(phosphine)rhodium complexes, but complexes with one or three phosphines may also be involved. The involvement of several catalytic cycles which differ in the number of phosphine ligands bound to rhodium is consistent with the increased selectivity observed at higher phosphine concentrations. The catalytic cycle with two coordinated phosphine ligands is proposed to be more selective for straight-chain aldehyde than cycles with fewer phosphine ligands. Increasing CO pressure results in a decrease in straight-chain aldehyde selectivity and is consistent with a decreased concentration of bis(phosphine)rhodium complexes at higher CO pressure. For detailed mechanistic studies, chelating phosphines are attractive since they should give an enhanced preference for bis(phosphine)rhodium complexes.[4]

The regiochemistry of hydroformylation of terminal alkenes is determined in the step that converts a five-coordinate H(alkene)Rh(CO)L_2 into either a primary or secondary four-coordinate (alkyl)Rh(CO)L_2 (Scheme I). To understand and control regioselectivity, it is important to know the detailed structure of the key five-coordinate H(alkene)Rh(CO)L_2 intermediate. Two monodentate phosphine ligands might occupy two equatorial, two apical, or one equatorial and one apical site in a trigonal bipyramidal intermediate. For L = PPh_3, Brown's NMR studies showed an 85:15 diequatorial/apical–equatorial mixture of isomers of HRh$(CO)_2(PPh_3)_2$.[5] At room temperature these isomers are in rapid equilibrium.

In an effort to generate rhodium complexes in which the phosphines have a greatly enhanced preference for occupying specific sites in trigonal bipyramids, we have investigated the use of chelating diphosphines in which the chelate backbone restricts the P–M–P bite angle. For example, $Ph_2PCH_2CH_2PPh_2$ (DIPHOS) is known from many X-ray structure determinations to have a strong preference for a P–M–P bite angle of near 90° and would be expected to selectively span apical and equatorial sites in a trigonal bipyramid. We wanted to study other chelating diphosphines which would have a preferred bite angle near 120° and which would be expected to preferentially occupy two equatorial sites on a trigonal bipyramid. Catalysts with such 120° bite angles chelates might show quite different regioselectivity than catalysts with 90° bite angle chelates.

Very high regioselectivity for formation of straight-chain aldehydes was achieved by Kodak using rhodium catalysts and the BISBI chelating ligand (**1**).[6] Examination of molecular models of Rh(BISBI) complexes indicated that the chelate bite angle was much greater than 90°. This suggested that ligands with large bite angles might be important in controlling regioselectivity and stimulated our interest in studying the effect of wide bite angle ligands on regioselectivity in hydroformylation.

To select chelates with wide bite angles for study, we have used molecular mechanics to estimate the "natural bite angle" of chelates and their flexibility.[7] We have defined the "natural bite angle" as the preferred chelation angle determined only by ligand backbone constraints and not by metal valence angles. This definition is independent of any electronic preference for a specific bite angle imposed by the metal center and is solely based on steric considerations. The natural bite angle is calculated by minimizing the strain energy of the M(diphosphine) fragment with a P–M–P bending force constant of 0 kcal mol^{-1} rad^{-2}. By fixing the bite

(1) (a) Parshall, G. W. *Homogeneous Catalysis: The Applications and Chemistry of Catalysis by Soluble Transition Metal Complexes*; Wiley: New York, 1980. (b) Thatchenko, I. In *Comprehensive Organometallic Chemistry*; Wilkinson, G., Stone, F. G. A., Abel, E. W., Eds.; Pergamon: Oxford, 1982; Vol. 8, p 101. (c) Tolman, C. A.; Faller, J. W. In *Homogeneous Catalysis with Metal Phosphine Complexes*; Pignolet, L. H., Ed.; Plenum: New York, 1983; pp 81–109. (d) Wender, R. I.; Pino, P. In *Organic Syntheses via Metal Carbonyls*; Wiley Interscience: New York, 1977; Vol. 2, pp 136–197.
(2) (a) Evans, D.; Osborn, J. A.; Wilkinson, G. *J. Chem. Soc. A* **1968**, 3133. (b) Yagupsky, G.; Brown, C. K.; Wilkinson, G. *J. Chem. Soc. A* **1970**, 1392. (c) Brown, C. K.; Wilkinson, G. *J. Chem. Soc. A* **1970**, 2753.
(3) Pruett, R. L. *Ann. N.Y. Acad. Sci.* 1977, *295*, 239.
(4) (a) Sanger, A. R.; Schallig, L. R. *J. Mol. Catal.* **1978**, *3*, 101. (b) Hayashi, T.; Tanaka, M.; Ikeda, Y.; Ogata, I. *Bull. Chem. Soc.* **1979**, *52*, 2605. (c) Hughes, O. R.; Unruh, J. D. *J. Mol. Catal.* **1981**, *12*, 71.
(5) Brown, J. M.; Kent, A. G. *J. Chem. Soc., Perkin Trans. 2* **1987**, 1597.
(6) Devon, T. J.; Phillips, G. W.; Puckette, T. A.; Stavinoha, J. L.; Vanderbilt, J. J. U.S. Patent 4,694,109.
(7) Casey, C. P.; Whiteker, G. T. *Isr. J. Chem.* **1990**, *30*, 299.

0002-7863/92/1514-5535$03.00/0

Scheme I

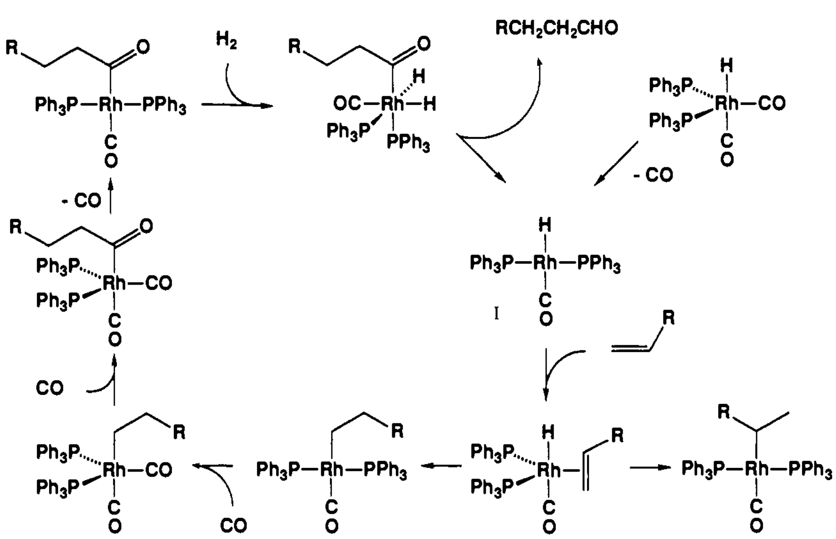

angle at various values by using a large bending force constant and then calculating the strain energy, potential energy diagrams can be constructed. These potential energy diagrams allow an estimation of the flexibility of the diphosphine chelate.

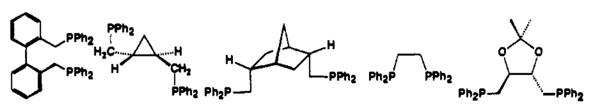

BISBI, 1 T-BDCP, 2 3 DIPHOS DIOP

Molecular mechanics calculations of Rh(BISBI) using a 2.315 Å Rh–P distance confirmed our initial expectations from examination of molecular models. The natural bite angle for the rhodium complex of BISBI (**1**) was found to be 113°, and the potential energy diagram (Figure 1) suggested that bite angles between 92° and 155° could be achieved with less than 3 kcal mol^{-1} additional strain energy. Thus, the BISBI ligand is a very flexible ligand and can accommodate a wide range of angles. The rhodium complex of the cyclopropyl diphosphine chelate T-BDCP (**2**) used by Rhone-Poulenc[8] was calculated to have a wide natural bite angle of 107° and was also somewhat flexible: bite angles between 93 and 131° were calculated to be accessible with less than 3 kcal mol^{-1} excess strain energy. Calculations of rhodium complexes of diphosphine **3** indicated a natural bite angle of 123° and an accessibility of bite angles between 110° and 145° with less than 3 kcal mol^{-1}; this provided incentive for us to develop a synthesis of this new chelate.[9] Other ligands selected for study included DIOP and DIPHOS. DIOP had a calculated natural bite angle of 102° and accessibility of bite angles between 90° and 120° with less than 3 kcal mol^{-1} excess strain energy; observed bite angles for DIOP complexes between 90° to 107° have been measured by X-ray crystallography.[10] DIPHOS had a calculated natural bite angle of 85° and accessibility of bite angles between 70° and 95° with less than 3 kcal mol^{-1} excess strain energy; observed bite angles for DIPHOS complexes between 84° and 90° have been measured by X-ray crystallography.[11]

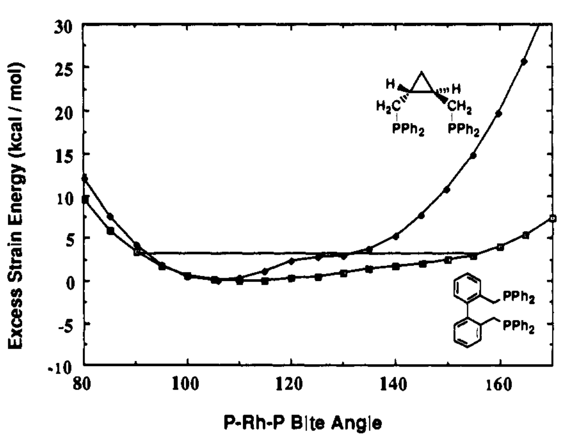

Figure 1. Calculated excess strain energy of Rh(BISBI) and of Rh-(T-BDCP) as a function of the P–Rh–P bite angle. The horizontal line is drawn 3 kcal mol^{-1} above the energy minimum.

The chelates chosen for study were all alkyldiphenylphosphines which were expected to have similar electronic properties. From the start, we realized that it would be difficult to separate steric and electronic effects resulting from the effect of the size of the chelate bite angle. Chelates with bite angles near 120° would be expected to occupy diequatorial sites that are electronically different from the apical–equatorial sites occupied by 90° bite angle chelates. A wide bite angle provides a mechanism for enlarging the effective steric bulk of a ligand.[12] It was known that increasing the steric bulk of monodentate ligands tended to lead to higher regioselectivity for hydroformylation to straight-chain aldehydes.[13]

Here we report the syntheses, structure, and dynamics of rhodium complexes with wide bite angles. We also report an increase in regioselectivity that accompanies the expansion of the bite angle of the diphosphine ligand.

Results

Prior to studying the effect of wide bite angle chelates on hydroformylation selectivity, we set out to learn as much as possible about the solid-state and solution structures of rhodium complexes of BISBI and T-BDCP. These chelates were expected to lock key intermediates into geometries with large bite angles. A comparison with the solution structure of $(Ph_3P)_2Rh(CO)_2H$ would indicate the nature of the changes brought about by chelation at wide bite angles.

Brown has used NMR spectroscopy to determine the solution structures of unconstrained, monodentate phosphine rhodium hydroformylation catalysts.[5] The reaction of $(PPh_3)_3Rh(CO)H$ (**4**) with CO gave an 85:15 mixture of $(Ph_3P)_2Rh(CO)_2H$ isomers **5**-ee and **5**-ea. Treatment of this mixture with an alkene gave a single isomer of the acyl complex $(Ph_3P)_2(CO)_2Rh(COR)$ (**6**), which was found to have one equatorial and one apical phosphine

(8) Aviron-Violet, P.; Colleuille, Y.; Varagnat, J. *J. Mol. Catal.* **1979**, *5*, 41.

(9) Casey, C. P.; Whiteker, C. P. *J. Org. Chem.* **1990**, *55*, 1394.

(10) (a) Ball, R. G.; Trotter, J. *Inorg. Chem.* **1981**, *20*, 261. (b) Ball, R. G.; James, B. R.; Mahajan, D.; Trotter, J. *Inorg. Chem.* **1981**, *20*, 254.

(11) Battaglia, L. P.; Delledonne, D.; Nardelli, M.; Pelizzi, C.; Predieri, G.; Chiusoli, G. P. *J. Organomet. Chem.* **1987**, *330*, 101.

(12) Tolman, C. A.; Seidel, W. C.; Gosser, L. W. *J. Am. Chem. Soc.* **1974**, *96*, 53.

(13) Pruett, R. L.; Smith, J. A. *J. Org. Chem.* **1969**, *34*, 327.

Table I. Comparison of Bond Lengths and Angles for (BISBI)Rh(PPh$_3$)(CO)H·CH$_2$Cl$_2$ (**7**·CH$_2$Cl$_2$), (BISBI)Ir(CO)$_2$H·$^1/_2$O(CHMe$_2$)$_2$ (**11**·$^1/_2$O(CHMe$_2$)$_2$), and (PPh$_3$)$_3$Rh(CO)H (**4**)

(BISBI)Rh(PPh$_3$)(CO)H		(BISBI)Ir(CO)$_2$H		(PPh$_3$)$_3$Rh(CO)H	
		Bond Lengths (Å)			
Rh–P(1)	2.285 (1)	Ir–P(1)	2.306 (3)	Rh–P(1)	2.336 (8)
Rh–P(2)	2.318 (1)	Ir–P(2)	2.300 (3)	Rh–P(3)	2.315 (8)
Rh–P(3)	2.318 (1)			Rh–P(2)	2.316 (9)
Rh–C(57)	1.895 (5)	Ir–C(1CO)	1.892 (12)	Rh–C	1.829 (28)
		Ir–C(2CO)	1.900 (12)		
		Bond Angles (deg)			
P(1)–Rh–P(2)	124.8 (1)	P(1)–Ir–P(2)	117.9 (1)	P(1)–Rh–P(3)	120.5 (3)
P(1)–Rh–P(3)	122.6 (1)			P(1)–Rh–P(2)	115.8 (2)
P(2)–Rh–P(3)	108.0 (1)			P(2)–Rh–P(3)	116.7 (3)
P(1)–Rh–C(57)	95.3 (1)	P(1)–Ir–C(2CO)	93.4 (4)	P(1)–Rh–CO	94.8 (8)
P(2)–Rh–C(57)	93.3 (1)	P(2)–Ir–C(2CO)	98.3 (4)	P(3)–Rh–CO	97.8 (8)
P(3)–Rh–C(57)	103.1 (1)	P(1)–Ir–C(1CO)	125.8 (4)	P(2)–Rh–CO	104.0 (8)
		P(2)–Ir–C(1CO)	112.2 (4)		

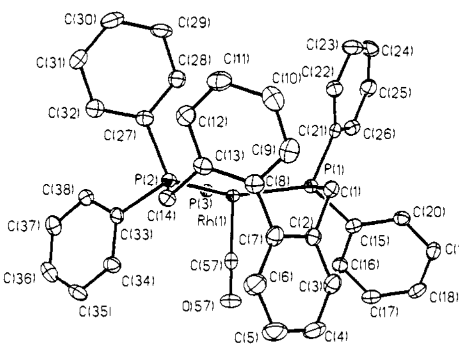

Figure 2. X-ray structure and numbering scheme for (BISBI)Rh(PPh$_3$)(CO)H (**7**·CH$_2$Cl$_2$). The phenyl groups on P(3), PPh$_3$, have been omitted for clarity.

ligand. Brown's observations suggest that hydroformylation intermediates may adopt a variety of geometries, and the number of possible structures might be reduced by using a chelating ligand with a known preferred bite angle.

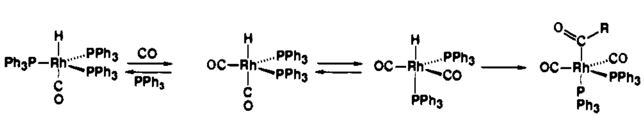

4 5-ee 5-ae 6

(BISBI)Rh(PPh$_3$)(CO)H (7). Because of the extremely high n:i ratios seen for BISBI, the solid-state and solution structures of its rhodium complexes were studied in great detail. The reaction of (Ph$_3$P)$_3$Rh(CO)H (**4**) with BISBI in CH$_2$Cl$_2$ produced (BISBI)Rh(PPh$_3$)(CO)H (**7**) as a crystalline solid in 90% yield.

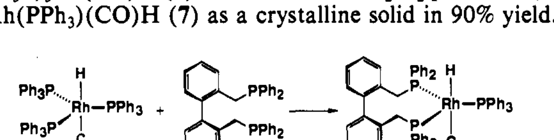

4 7

The X-ray crystal structure of **7**·CH$_2$Cl$_2$ (Figure 2, Table I) reveals a distorted trigonal bipyramidal geometry about rhodium. The BISBI ligand occupies two equatorial sites with a P–Rh–P bite angle of 124.8 (1)°. The P–Rh–P angles between the BISBI ligand and the equatorial triphenylphosphine are 122.6 (1)° and 108.0 (1)°. The Rh atom resides only slightly out of the equatorial plane defined by the three phosphorus atoms and is displaced toward the apical carbonyl ligand. Although the hydride ligand was not located in the X-ray crystal structure, we believe it occupies the site trans to the apical CO ligand. The carbonyl ligand occupies an apical site and is bent toward the triphenylphosphine ligand with a Ph$_3$P–Rh–CO angle of 103.1 (1)°. Table I shows that there are only slight differences between comparable bond lengths and angles of (Ph$_3$P)$_3$Rh(CO)H[14] (**4**) and (BISBI)Rh(PPh$_3$)(CO)H·CH$_2$Cl$_2$ (**7**·CH$_2$Cl$_2$).

The similarity of the BISBI P–Rh–P bite angle of **7**·CH$_2$Cl$_2$ to the PPh$_3$ P–Rh–P angles of **4** suggests that electronic considerations are responsible for the ~120° angles between the phosphines in these two complexes. The BISBI ligand is quite flexible and accommodates a range of bite angles between 152° in (BISBI)Fe(CO)$_3$[15] and 104° in (BISBI)Mo(CO)$_4$.[16] In (R$_3$P)$_2$Fe(CO)$_3$ complexes, the phosphine ligands have an electronic preference for the apical positions.[17] In (BISBI)Fe(CO)$_3$, the bite angle expands well beyond the natural bite angle of 113° to 152° in an apparent attempt to achieve apical coordination that is thwarted by the excess strain energy of very wide bite angles. In (BISBI)Mo(CO)$_4$, the bite angle is compressed below the natural bite angle of 113° to 104° to coordinate to cis octahedral sites. These three structures indicate that BISBI prefers a relatively wide bite angle but is also a relatively flexible ligand which readily accommodates bite angles in the 100–160° range.

The presence of a hydride ligand in **7** was confirmed by NMR spectroscopy. In the ^{1}H NMR spectrum of **7** in CD$_2$Cl$_2$, the rhodium hydride resonance appeared as a slightly broadened triplet of doublets at δ −10.43 (td, J_{HP} = 16, 6 Hz). The relatively small phosphorus–hydrogen coupling constants are consistent with a structure in which an apical hydride is cis to three equatorial phosphines. The value of J_{RhH} was estimated to be less than 2 Hz from the line width of the hydride resonance. The ^{31}P{^{1}H} NMR spectrum of **7** in CD$_2$Cl$_2$ at −40 °C consisted of an AMXRh pattern due to complexed PPh$_3$ and the two diastereotopic phosphorus atoms of the BISBI ligand of **7**.

Infrared spectroscopy allows an easy distinction to be made between cis and trans isomers of metal–carbonyl hydrides.[18] For cis M(CO)H compounds, symmetry does not allow interaction between ν_{MH} and ν_{CO}, and two unshifted bands are observed. Upon deuteration, the ν_{CO} band of M(CO)D appears at the same frequency as that for M(CO)H. For the trans isomer of M(CO)H, symmetry allows a resonance interaction between the ν_{CO} and ν_{MH} vibrations which is large because of the similar frequencies of the two vibrations. The interaction gives rise to two combination bands, one shifted to higher energy than that expected for noninteracting ν_{MH} and ν_{CO} vibrations and the other shifted to lower energy. This resonance interaction disappears upon deuteration since ν_{MD} and ν_{CO} are too different in energy to interact significantly. For the deuterated derivative, a single high-energy band due to a noninteracting ν_{CO} is seen at a frequency significantly shifted from its position in M(CO)H.

(14) LaPlaca, S. J.; Ibers, J. A. *Acta Crystallogr.* **1965**, *18*, 511.
(15) Casey, C. P.; Whiteker, G. T.; Campana, C. F.; Powell, D. R. *Inorg. Chem.* **1990**, *29*, 3376.
(16) Herrmann, W. A.; Kohlpainter, C. W.; Herdtweck, E.; Kiprof, P. *Inorg. Chem.* **1991**, *30*, 4271.
(17) For example, see: Allison, D. A.; Clardy, J.; Verkade, J. G. *Inorg. Chem.* **1972**, *11*, 2804.
(18) Vaska, L. *J. Am. Chem. Soc.* **1966**, *88*, 4100.

Scheme II

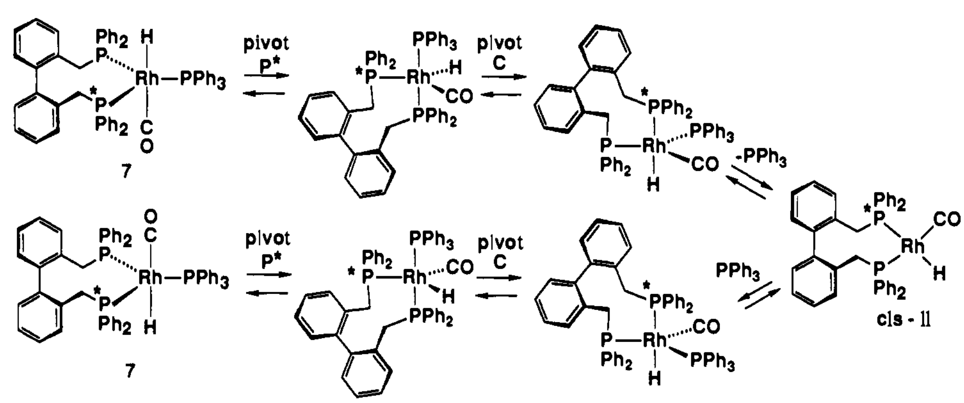

The IR spectrum of 7 in CH_2Cl_2 had bands at 2012 (s) and 1921 (m) cm^{-1} due to combination bands of ν_{RhH} and ν_{CO}. Deuteration of 7 was achieved by stirring a CH_2Cl_2 solution of 7 under 1 atm of D_2. The IR spectrum of **7d** had a single high-energy ν_{CO} band at 1969 cm^{-1}. The large shift of this band upon deuteration establishes that the hydride and CO ligands of 7 are trans to one another. This provides strong evidence that the solid-state geometry of 7 is maintained in solution.

The ^{13}C-labeled compound, 7-^{13}CO, was prepared from the reaction of BISBI with $(PPh_3)_3Rh(^{13}CO)H$ in CH_2Cl_2. In the ^1H NMR spectrum of 7-^{13}CO, the rhodium hydride appeared as a multiplet at δ −10.43 (dtd, J_{CH} = 40 Hz, $J_{PH} \approx 16$ Hz, $J_{P'H}$ = 6 Hz). The 40-Hz coupling between the hydride and the trans ^{13}CO in 7-^{13}CO is similar to the 38-Hz coupling observed by Brown for $(Ph_3P)_3Rh(^{13}CO)H$ (**4**).[5] In the ^{13}C NMR spectrum of 7-^{13}CO in CD_2Cl_2, the ^{13}CO ligand gave rise to a multiplet at δ 205.4 (tq, $J_{CH} = J_{RhC}$ = 42 Hz, J_{PC} = 11 Hz).

The hydroformylation mechanism proposed by Wilkinson involves phosphine dissociation from $(PPh_3)_3Rh(CO)H$ to give the coordinatively unsaturated intermediate $(PPh_3)_2Rh(CO)H$ (I) (Scheme I).[2] Oswald[19] and Brown[5] found rapid exchange between free PPh_3 and coordinated PPh_3 on **4** by ^{31}P NMR. Coalescence was seen near 60 °C, and dissociation of PPh_3 from **4** was found to have $\Delta G^{\ddagger}$ = 15.5 kcal mol^{-1} at 7 °C.

We studied the exchange of free PPh_3 (2 equiv) with 7 by $^{31}P\{^1H\}$ NMR and found rapid exchange of PPh_3 and no evidence for BISBI dissociation (Figure 3). At 30 °C, a sharp singlet at δ −4.4 for PPh_3 and an ABCRh pattern at δ 34–43 due to the three different coordinated phosphorus atoms of 7 were observed. As the temperature was increased, both resonances broadened and shifted in frequency. At 70 °C, the free PPh_3 signal was broad ($\omega_{1/2}$ = 350 Hz), the coordinated PPh_3 signal was too broad to observe, and resonances due to the two BISBI phosphorus atoms appeared as a sharp doublet (J_{PRh} = 159 Hz) at δ 38.7. The NMR equivalence of the two BISBI phosphorus atoms at high temperature requires a fluxional process that interchanges their environments. This process cannot involve BISBI dissociation from rhodium since coupling is maintained at high temperature. At 119 °C, a single very broad ($\omega_{1/2}$ = 2000 Hz) resonance at δ 6 was observed for rapidly exchanging free and coordinated PPh_3; the BISBI resonance remained a sharp doublet. Line shape analysis of these ^{31}P NMR spectra over the temperature range 30–119 °C gave rate constants for PPh_3 dissociation and allowed calculation of $\Delta G^{\ddagger}$ = 15.5 kcal mol^{-1} for PPh_3 dissociation from 7. Thus, the rate of PPh_3 dissociation from BISBI complex 7 is similar to that for dissociation from $(PPh_3)_3Rh(CO)H$ (**4**).

Our data were not precise enough to determine whether the activation energy for interchange of the BISBI phosphorus atoms was the same as the activation energy for PPh_3 exchange. We suggest that interchange of the BISBI phosphorus atoms occurs via the same planar 4-coordinate intermediate (BISBI)Rh(CO)H (*cis*-**II**) involved in PPh_3 exchange. The formation of *cis*-**II** is proposed to occur via loss of equatorial PPh_3 from a conformation of 7 in which BISBI spans an apical and an equatorial position. This conformation is readily accessible by the series of pseudorotations shown in Scheme II.

Two other mechanisms might also explain the interchange of the BISBI phosphorus atoms. First, loss of PPh_3 from the equatorial position of 7 would produce *trans*-**II**, in which BISBI spans the trans positions of the square planar complex. While such an intermediate would account for PPh_3 exchange, it does not allow exchange of the diastereotopic BISBI phosphorus atoms because one side of *trans*-**II** is blocked by the biphenyl linkage of the chelate. However, rotation of the Rh–H bond through the center of the chelate ring of *trans*-**II** would exchange the BISBI phosphorus atoms. Second, reversible dissociation of one of the BISBI phosphorus atoms to give a monodentate square planar complex **III** would interchange the environments of the BISBI phosphorus atoms. Generation of **III** would not result in loss of the P–Rh coupling. However, this mechanism requires the dissociation of a less labile alkyldiphenylphosphine ligand. We favor the mechanism shown in Scheme II since it only requires the dissociation of a more labile PPh_3 ligand and since the ^{31}P NMR spectrum provides evidence for rapid PPh_3 dissociation under these conditions.

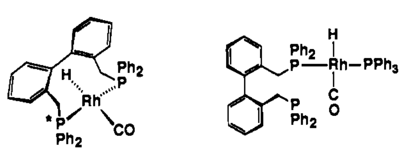

trans - II III

When a solution of 7 in CD_2Cl_2 was placed under 1 atm of CO at −30 °C, the ^1H NMR spectrum revealed a new rhodium hydride signal in addition to that of 7 in a 1:1.2 ratio. The new hydride resonance at δ −10.77 was a triplet (J_{PH} = 8 Hz) coupled to only two phosphorus atoms; the small value of J_{PH} is consistent with

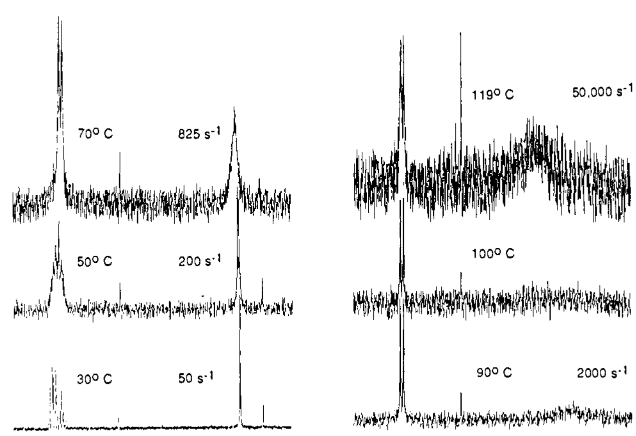

Figure 3. Variable-temperature $^{31}P\{^1H\}$ NMR spectra of (BISBI)Rh(PPh_3)(CO)H (7) in toluene-d_8. The exchange rates determined by line shape analysis using DNMR5 are shown next to each spectrum.

(19) Kastrup, R. V.; Merola, J. S.; Oswald, A. A. *Adv. Chem. Ser.* **1982**, *196*, 43.

Scheme III

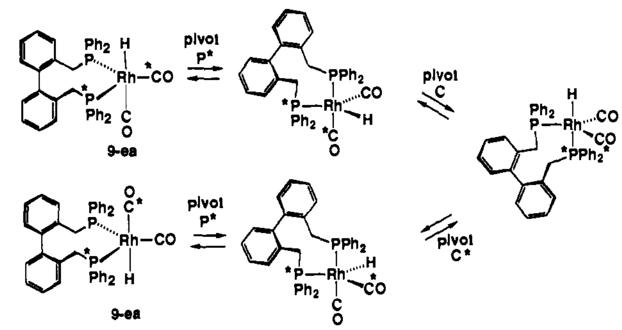

the hydride being cis to two phosphorus atoms. This triplet was assigned to (BISBI)Rh(CO)$_2$H (**9**), presumably formed by CO trapping of *cis*-**II**.

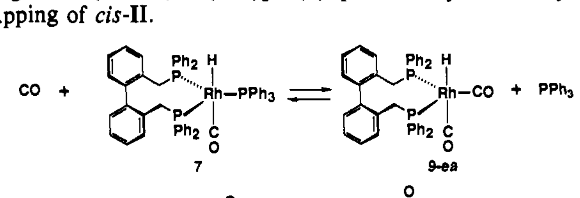

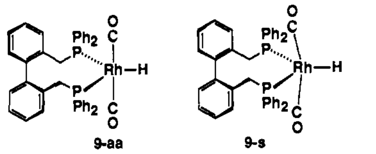

When a solution of **7** in CD_2Cl_2 was placed under 0.61 atm of ^{13}CO at −10 °C, a 1:1.2 mixture of monolabeled **7**-^{13}CO and doubly labeled **9**-^{13}CO was formed as determined by ^{1}H NMR spectroscopy. The hydride resonance of **9**-^{13}CO was coupled to two NMR equivalent ^{13}C carbons and to two NMR equivalent phosphorus atoms and appeared as a triplet of triplets at δ −10.77 (tt, J_{CH} = 16 Hz, J_{PH} = 8 Hz). The ^{13}C{^{1}H} NMR spectrum of **9**-^{13}CO exhibited a single carbonyl resonance at δ 199.2 (dt, J_{RhC} = 61 Hz, J_{PC} = 10 Hz). Both the ^{1}H and ^{13}C NMR spectra of **9**-^{13}CO were unchanged at −70 °C and were consistent with either a fluxional structure with one equatorial and one apical carbonyl (**9**-ea) or a structure with two equivalent carbonyl groups, such as one having two apical carbonyls **9**-aa or a structure distorted toward a square-based pyramid with trans carbonyls **9**-s.

The ambiguity about the geometry of **9** was resolved by infrared spectroscopy. A trans arrangement of carbonyls (**9**-aa) should give rise to only one intense carbonyl band in the infrared spectrum since the symmetric stretching vibration is IR inactive. For square pyramidal **9**-s, the high-energy symmetric stretch should be much less intense than the low-energy asymmetric stretch. For **9**-ea, the two carbonyl groups are not symmetry related, and two infrared active carbonyl bonds are expected. The deuteride **9**-d was studied to remove complications due to possible coupling of ν_{CO} and ν_{MH}. Compound **7**-d was prepared from a CH_2Cl_2 solution of **7** under 1 atm of D_2 and converted to **9**-d by bubbling carbon monoxide through the solution at −78 °C. The IR spectrum of **9**-d at −78 °C exhibited two carbonyl bands of equal intensity at 2017 and 1959 cm^{-1}, consistent only with **9**-ea. No band due to **7**-d was observed in this experiment with excess CO at 1 atm and low temperature. The infrared spectrum of **9** requires a structure with one apical and one equatorial carbonyl group, and the NMR equivalence of these carbonyls at −70 °C requires a rapid fluxional process to interchange the carbonyl ligands and to interchange the diastereotopic BISBI phosphorus atoms. The series of Berry pseudorotations shown in Scheme III accomplishes these interconversions.

In comparing (BISBI)Rh(CO)$_2$H (**9**) with $(Ph_3P)_2Rh(CO)_2H$ (**5**), we note that for **9** only a single isomer with equatorial phosphorus atoms is seen, while for **5** two isomers are seen: 85% of an isomer with equatorial phosphines **5**-ee and 15% of an equatorial–apical isomer **5**-ea. The NMR equivalence of the phosphorus atoms and of the carbonyls of **9** suggests that there is rapid equilibration with an apical–equatorial isomer.

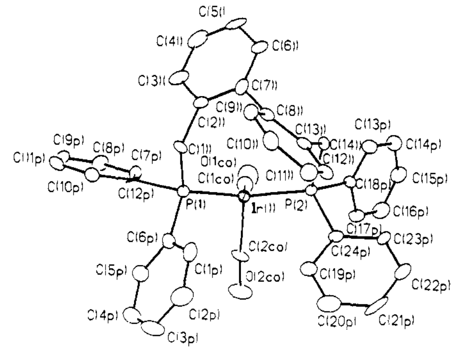

Figure 4. X-ray structure and numbering scheme for (BISBI)Ir(CO)$_2$H (**11**·$^1/_2$O(CHMe$_2$)$_2$).

The solution of **9**-d prepared from **7** and CO was stable at 25 °C for more than 30 min, but replacement of the CO atmosphere by nitrogen resulted in decarbonylation and reformation of **7**. Because we were unable to isolate rhodium dicarbonyl complex **9** due to its instability in the absence of CO, we made an effort to synthesize and isolate its iridium analog, (BISBI)Ir(CO)$_2$H (**11**). The reaction of $(Ph_3P)_3Ir(CO)H$[20] and BISBI in CH_2Cl_2 gave (BISBI)Ir(PPh$_3$)(CO)H (**10**) as a yellow solid in 84% yield. The reaction of **10** in toluene/ethanol under 1 atm of CO for 18 h gave (BISBI)Ir(CO)$_2$H (**11**) as a stable, pale yellow solid in 73% yield. As in the case of the rhodium complex (BISBI)Rh(CO)$_2$H (**9**), the NMR and IR spectra of iridium complex **11** were consistent with a fluxional structure with one apical and one equatorial CO.

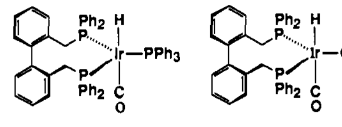

Crystallization of **11** from CH_2Cl_2/diisopropyl ether gave single crystals of **11**·$^1/_2$O(CHMe$_2$)$_2$. The X-ray crystal structure of **11**·$^1/_2$O(CHMe$_2$)$_2$ (Figure 4, Table I) shows one equatorial and one apical CO and confirms the infrared assignment of structure. The BISBI ligand of **11** spans equatorial sites with a bite angle of 117.9°, which is slightly smaller than the 124.8° bite angle of (BISBI)Rh(PPh$_3$)(CO)H (**7**). The similarity of these bite angles indicates that the electronic structure of the trigonal bipyramidal complexes is largely responsible for controlling the relatively flexible bite angles of BISBI.

(T-BDCP)Rh[P(C$_6$H$_4$-*p*-CH$_3$)$_3$](CO)H (12). Optically active diphosphine **2** (T-BDCP) was previously synthesized and used for rhodium-catalyzed asymmetric hydrogenations by Rhone-Poulenc.[8] Recently, we reported the X-ray crystal structure of racemic (T-BDCP)Fe(CO)$_3$, which has the diphosphine coordinated to equatorial sites of a trigonal bipyramid,[15] and found a P–Fe–P bite angle of 123.9°, which suggested that **2** was a selective di-equatorial ligand.

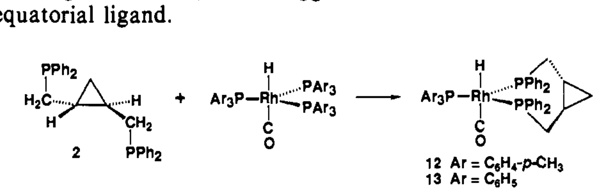

The solution structures of T-BDCP rhodium complexes were studied in somewhat less detail than those of the BISBI complexes because of problems with stability and purification. The reaction of racemic **2** with Rh[P(C$_6$H$_4$-*p*-CH$_3$)$_3$]$_3$(CO)H in methylene chloride produced the compound (T-BDCP)Rh[P(C$_6$H$_4$-*p*-CH$_3$)$_3$](CO)H (**12**) as a light yellow solid. Attempts to remove excess tri-*p*-tolylphosphine from complex **12** by recrystallization or chromatography were unsuccessful. ^{1}H NMR spectra of a 1:1

(20) Wilkinson, G. *Inorg. Synth.* **1972**, *13*, 126.

mixture of **12** and $P(C_6H_4\text{-}p\text{-}CH_3)_3$ in CD_2Cl_2 exhibited a high-field multiplet at δ −10.42 (qd, J_{PH} = 16 Hz, J_{RhH} = 2 Hz), assigned to the rhodium hydride of **12**. The $^{31}P\{^1H\}$ NMR spectrum exhibited an ABCRh pattern due to **12** (δ 36.8, 37.5, 38.2, all J_{PP} = 123 Hz, all J_{RhP} = 152–155 Hz) and a singlet at δ −7.5 due to free $P(C_6H_4\text{-}p\text{-}CH_3)_3$. The IR spectrum of **12** had two bands for resonance interaction of ν_{CO} and ν_{MH} at 1989 (s) and 1908 (m) cm^{-1}. Upon deuteration under 1 atm of D_2, the **12**-d which was formed gave rise to a single band at 1955 cm^{-1}. The shift in the carbonyl stretching frequency upon isotopic substitution requires that H and CO occupy trans positions. The NMR and IR spectra of **12** are consistent with a structure similar to that of **4** and **7** in which three phosphines lie in the equatorial plane of a trigonal bipyramid.

Exchange of phosphine with a T-BDCP complex was studied by ^{31}P NMR spectroscopy using the PPh_3 analog (T-BDCP)-$Rh(PPh_3)(CO)H$ (**13**), which was synthesized from **2** and $(Ph_3P)_3Rh(CO)H$ in CH_2Cl_2. Unfortunately, as in the case of **12**, recrystallization failed to remove excess phosphine. At 22 °C, the $^{31}P\{^1H\}$ NMR spectrum of a 2:1 mixture of PPh_3 and **13** in toluene-d_8 consisted of a singlet at δ −4.4 due to PPh_3 and an ABMRh pattern between δ 36 and 42 due to **13**. As the temperature was increased, the free PPh_3 resonance began to broaden, while the complexed phosphorus resonances remained sharp. This behavior suggests that PPh_3 is being broadened by an unobserved species and that this exchange mechanism does not involve complex **13**. At 107 °C, the free PPh_3 signal ($\omega_{1/2}$ = 650 Hz) and the coordinated PPh_3 signal ($\omega_{1/2}$ = 450 Hz) were broadened by exchange, and resonances due to the T-BDCP phosphorus atoms appeared as a broadened doublet (J_{PRh} = 173 Hz) at δ 37, indicative of rapid interchange of the environment of the diastereotopic T-BDCP phosphorus atoms. The observation that rhodium–phosphorus coupling is maintained at 107 °C indicates that T-BDCP does not dissociate from rhodium during the fluxional process. The broadening of PPh_3 at lower temperatures makes this data less reliable than that obtained with **7**. These observations are consistent with fast dissociation of PPh_3 from **13** at elevated temperature with no evidence for dissociation of the T-BDCP ligand. Qualitatively, the rate of the PPh_3 exchange with the T-BDCP complex **13** is substantially slower than PPh_3 exchange with BISBI complex **7**.

An attempt to form $(T\text{-}BDCP)Rh(CO)_2H$ (**14**) by exposure of a solution of $(T\text{-}BDCP)Rh[P(C_6H_4\text{-}p\text{-}CH_3)_3](CO)H$ (**12**) to 1 atm of CO in CH_2Cl_2 at −15 °C led to the observation of a new rhodium hydride. At −15 °C, the ^1H NMR spectrum indicated a 1.6:1 ratio of **12** to a new hydride resonance at δ −9.87 (td, J_{PH} = 16 Hz, J_{RhH} = 6 Hz) assigned to $(T\text{-}BDCP)Rh(CO)_2H$ (**14**). Upon warming to 25 °C, the hydride resonance of **14** disappeared with a time for half-reaction of 10 min, and a new resonance appeared at δ 4.5 (s, assigned to H_2). The $^{31}P\{^1H\}$ NMR spectrum of the decomposed solution had a doublet at δ 16.5 (J_{RhP} = 125 Hz), and the IR spectrum had a single carbonyl band at 1726 cm^{-1}. This data suggests that **14** decomposed by loss of CO and H_2 to form the dimer $[(T\text{-}BDCP)Rh]_2(\mu\text{-}CO)_2$ (**15**). Wilkinson[21] and Hodgson[22] have fully characterized the related PPh_3 complex $[(Ph_3P)_2Rh]_2(\mu\text{-}CO)_2$. Thus, $(T\text{-}BDCP)Rh(CO)_2H$ (**14**) is substantially less stable than $(BISBI)Rh(CO)_2H$ (**9**).

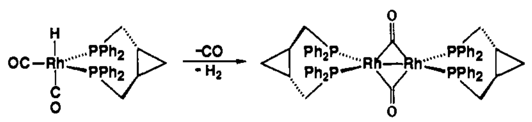

14 15

1-Hexene Hydroformylation Studies. Hydroformylation of 1-hexene was carried out at 34 °C under 6 atm of 1:1 H_2/CO using a 4 mM solution of 1:1 Rh/diphosphine. The production of heptanal and 2-methylhexanal was monitored by gas chromatography. $(Diphosphine)Rh(CO)_2H$ catalyst solutions were prepared from $(acac)Rh(CO)_2$ and chelating diphosphine ligands under 1:1 CO/H_2. This catalyst preparation from a phosphine-free rhodium starting material avoided complications due to additional phosphine ligands and was used recently by Trzeciak and Ziolkowski to study the hydroformylation of 1-hexene with Rh complexes of triaryl phosphites.[23,24]

Table II. Hydroformylation of 1-Hexene with Rhodium–Diphosphine Catalysts

diphosphine	turnover rate[a]	n:i[b]	calculated (diphosphine)Rh bite angle
BISBI (**1**)	29.4	66.5	112.6
T-BDCP (**2**)	3.7	12.1	106.6
DIOP	6.4	8.5	102.2
DIPHOS	1.1	2.1	84.5
norbornyl (**3**)	9.3	2.9	126.1

[a] Turnover rate = [moles aldehyde] × [moles Rh]$^{-1}$ h^{-1}. [b] n:i = moles heptanal:moles 2-methylhexanal.

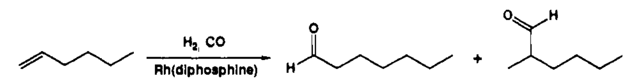

The results of rhodium-catalyzed hydroformylation of 1-hexene in the presence of chelating diphosphines with different P–M–P bite angles are shown in Table II. Turnover rates were determined by gas chromatography and were relatively constant over >50% conversion or >300 turnovers. Normal:iso (n:i) ratios of heptanal:2-methylhexanal did not vary significantly over the course of the reaction.

The diphosphine ligands used in the hydroformylation experiments have two alkyldiphenylphosphine units and should have similar electronic properties. Differences in hydroformylation selectivity should, therefore, be due to differences in steric effects and bite angles. Hydroformylation of 1-hexene in the presence of DIPHOS, a relatively rigid chelate with observed P–M–P bite angles near 90°, resulted in the formation of heptanal and 2-methylhexanal in a 2.1:1 n:i ratio.

The DIOP ligand has been used for enantioselective hydrogenation and hydroformylation of alkenes. DIOP complexes exhibit P–M–P bite angles in the range of 90° to 107°.[10] Hydroformylation of 1-hexene in the presence of DIOP gave an 8.5:1 n:i ratio of aldehydes.

Cyclopropyl diphosphine T-BDCP (**2**) forms an $Fe(CO)_3$ complex with an observed bite angle of 123.6°.[15] Rhodium-catalyzed hydroformylation of 1-hexene in the presence of **2** resulted in a high 12.1:1 n:i ratio of aldehydes.

The BISBI ligand **1** has been reported to give high selectivity for normal aldehyde formation in rhodium-catalyzed propene hydroformylation.[6] Use of BISBI for hydroformylation of 1-hexene led to the formation of aldehyde products with a very high 66.5:1 n:i ratio of aldehydes.

The norbornyl diphosphine **3** was calculated to have a natural bite angle of 126.1°. Hydroformylation of 1-hexene in the presence of **3** led to a low 2.9:1 n:i ratio of aldehydes. Although this diphosphine has a large calculated bite angle, we have been unable to isolate monomeric metal complexes of **3** and believe that **3** may not act as a chelating ligand.

Discussion

It is generally believed that the regiochemistry of rhodium-catalyzed hydroformylation is determined at the stage of Rh–H addition to the alkene. The conversion of a rhodium-hydride-alkene complex to a primary or secondary rhodium-alkyl complex is so rapid that direct observation of the rhodium-alkene-hydride complex has not been possible. The geometry and steric environment of the rhodium-alkene-hydride complex and of the initially produced 4-coordinate alkyl-rhodium intermediate are likely to be very important in controlling the regiochemistry of the

(21) Evans, D.; Yagupsky, G.; Wilkinson, G. *J. Chem. Soc. A* **1968**, 2660.
(22) Singh, P.; Dammann, C. B.; Hodgson, D. J. *Inorg. Chem.* **1973**, *12*, 1335.
(23) Trzeciak, A. M.; Ziolkowski, J. J. *J. Mol. Catal.* **1988**, *48*, 319.
(24) This system was first employed at Union Carbide. Pruett, R. L.; Smith, J. A. U.S. Patent 3,527,809.

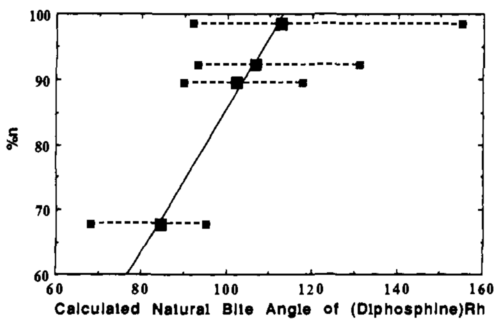

Figure 5. Plot of % *n*-aldehyde vs calculated natural bite angle of (diphosphine)Rh. Horizontal bars indicate the range of bite angles accessible with <3 kcal additional calculated strain energy.

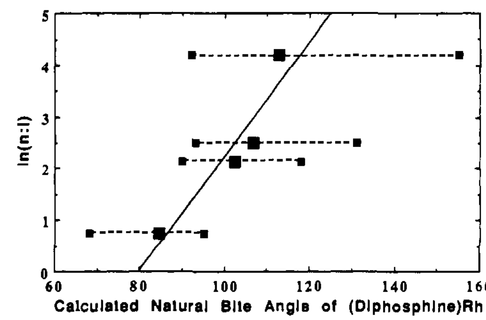

Figure 6. Plot of ln (n:i) vs calculated natural bite angle of (diphosphine)Rh. Horizontal bars indicate the range of bite angles accessible with <3 kcal additional calculated strain energy.

reaction and are presumably affected by the natural bite angle of a chelating ligand.

Several limiting geometries can be considered for the 5-coordinate rhodium–alkene–hydride complex. The chelating diphosphine could span an apical and an equatorial position of a trigonal bipyramid as in **AE**. Chelates such as DIPHOS with natural bite angles near 90° would stabilize **AE**. Alternatively, the chelating diphosphine might span two equatorial positions in a trigonal bipyramid as in **EE**. Chelates with natural bite angles near 120° would stabilize **EE**. A third limiting structure is one in which the chelating diphosphine spans trans basal positions in a square-based pyramid BB. This limiting geometry would be stabilized by chelates with natural bite angles greater than 120°. It should be remembered that there is a continuum of observed structures for 5-coordinate intermediates that lie along the reaction coordinate that interconverts trigonal bipyramids via a square-based pyramidal geometry in the Berry pseudorotation.

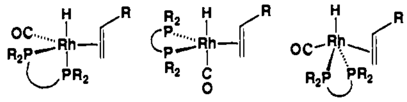

AE **EE** **BB**

While the actual bite angle of the diphosphine ligand in the rhodium–alkene–hydride intermediate may be important in controlling regiochemistry, it is not directly available for any complex. Bite angles for some complexes like (BISBI)Rh(PPh_3)(CO)H (**7**) are available but not for an entire series of compounds. The actual bite angle should depend on the natural bite angle and on displacements caused by electronic preferences and steric interactions with the other ligands. For the relatively small hydride, CO, and alkene ligands, the calculated natural bite angle may be well correlated with the actual bite angle. To explore the relationship between the regioselectivity of hydroformylation and the calculated natural bite angle of (diphosphine)Rh complexes, we plotted the %n vs calculated natural bite angle (Figure 5) and ln (n:i) vs calculated natural bite angle (Figure 6). To give an estimate of the ligand flexibilities, bars indicating the range of bite angles accessible with <3 kcal additional calculated strain energy are shown.

The actual bite angles for BISBI and T-BDCP rhodium–alkene–hydride complexes may be somewhat larger than the natural bite angles because of an electronic preference to widen the angle to near the 120° angle of diequatorial positions on a trigonal bipyramid. For example, the calculated natural bite angle of (BISBI)Rh is 113°, but the observed bite angle in (BISBI)Rh(PPh_3)(CO)H (**7**) is 125° and in (BISBI)Ir$(CO)_2$H (**11**) is 118°.

Because the norbornyl diphosphine **3** is apparently unable to form stable chelates (we have been unable to characterize monomeric complexes of **3**), this chelate is not included in the correlations shown in Figures 5 and 6. The observed n:i for **3** of 2.9:1 is much lower than that expected for a calculated natural bite angle of 126° and is similar to that seen for nonchelating phosphines. Yamamoto has reported that rhodium-catalyzed hydroformylation of 1-octene in the presence of norbornyl diphosphine **3** produced a 1.2:1 n:i ratio of aldehydes under higher total pressure.[25]

The reasons for the increased regioselectivity of hydroformylation seen for chelates with large natural bite angles are not known. The BISBI and T-BDCP ligands which show the highest regioselectivity for *n*-aldehyde formation not only have relatively wide natural bite angles but also are quite flexible and can accommodate a wide range of bite angles with little additional strain energy. One possible reason for the increased regioselectivity seen for wide bite angle phosphines might be that these chelates preferentially occupy diequatorial sites in the rhodium–alkene–hydride intermediate **EE** and that this geometry has higher selectivity for *n*-aldehyde formation than geometries with apical–equatorial chelates such as **AE**. Alternatively, the large bite angle of phosphines might simply serve to increase the effective steric bulk of the diphosphine,[12] and a good correlation of high n:i regioselectivity and steric size of monodentate ligands has been observed.[13] To begin to distinguish between these possibilities, we will need to design diphosphines having similar bite angles and electronically similar substituents but with different steric size of substituents at phosphorus. We also plan to study ligands with similar bite angles but different calculated flexibilities.

Conclusion

Rhodium complexes of two diphosphine ligands with wide P–Rh–P bite angles were synthesized, and their solution structures were probed spectroscopically. The X-ray structure of (BISBI)Rh(PPh_3)(CO)H·CH_2Cl_2 revealed chelation of BISBI at equatorial sites of the trigonal bipyramidal rhodium with a bite angle of 125°. Comparison of this compound with (BISBI)Fe$(CO)_3$, which has a bite angle of 152°, and with (BISBI)Mo$(CO)_4$, which has a bite angle of 104°, suggested that BISBI formed complexes with wide bite angles but was a flexible ligand. A correlation was observed between the regioselectivity of the rhodium-catalyzed hydroformylation of 1-hexene and the calculated natural bite angle of chelating diphosphines.

Experimental Section

General. ^{1}H NMR spectra were measured on a Bruker WP270 or AM500 spectrometer. ^{13}C NMR spectra were obtained on a Bruker AM500 spectrometer operating at 125.76 MHz. ^{31}P NMR spectra were obtained on an AM500 instrument (202.46 MHz) and were referenced to external 85% H_3PO_4. Line shape analysis was performed using the program DNMR5.[26] Infrared spectra were measured on a Mattson Polaris (FT) spectrometer. Low-temperature infrared spectra were obtained using a Beckman-RICC VLT-2 variable-temperature cell. GC–MS was performed on a Carlo-Erba gas chromatograph interfaced to a Kratos MS-25 mass spectrometer. Gas chromatography was performed on either a Hewlett-Packard 5890A or 5700 gas chromatograph connected to an HP3390A integrator.

CH_2Cl_2 and CD_2Cl_2 were distilled from CaH_2. Hexane, benzene, and toluene-d_8 were distilled from purple solutions of sodium and benzophenone. Methanol was dried over magnesium turnings and distilled prior to use. 1-Hexene (99%) was distilled prior to use.

All air-sensitive materials were handled with use of standard high vacuum manifold and inert atmosphere glove box techniques. $(Ph_3P)_3RhCl$,[27] (acac)Rh$(CO)_2$,[28] $[(CH_3C_6H_4)_3P]_3$Rh(CO)H,[29]

(25) Miyazawa, M.; Momose, S.; Yamamoto, K. *Synlett* **1990**, 711.
(26) Stephenson, D. S.; Binsch, G. *QCPE Bull.* **1978**, *10*, 365.
(27) Osborn, J. A.; Wilkinson, G. *Inorg. Synth.* **1967**, *10*, 67.

$(Ph_3P)_3Ir(CO)H$,[20] and $(Ph_3P)_3Rh(CO)H$[30] were prepared by literature methods. ^{13}CO (99.5% ^{13}C) was obtained from Monsanto Research Corporation. Analyzed mixtures of 1:1 CO/H_2 were obtained from Matheson Gas Products.

(BISBI)Rh(PPh$_3$)(CO)H·CH$_2$Cl$_2$ (7·CH$_2$Cl$_2$). A solution of $(Ph_3P)_3Rh(CO)H$ (654 mg, 0.712 mmol) and 2,2'-bis[(diphenylphosphino)methyl]-1,1'-biphenyl[6] (409 mg, 0.743 mmol) in 20 mL of CH_2Cl_2 was stirred for 3 h at 25 °C. The solvent was evaporated under vacuum. The resulting yellow solid was washed with 20 mL of methanol and filtered to give 7·CH_2Cl_2 (605 mg, 90%) as a yellow powder. A sample for elemental analysis was crystallized from 5:1 hexane/CH_2Cl_2: ^1H NMR (500 MHz, CD_2Cl_2) δ 7.8–5.9 (m, aromatic H), 4.3–3.4 (m, CH_2P), −10.46 (td, J_{PH} = 16, 6 Hz, RhH); $^{13}C\{^1H\}$ NMR (CD_2Cl_2) δ 205.0 (dq, J_{RhC} = 53 Hz, J_{PC} = 12 Hz, CO), 142.5 (d, J_{PC} = 28 Hz), 139.2 (d, J_{PC} = 32 Hz, 2,2' or ipso), 137.9, 136.5, 136.3, 136.1, 135.3, 133.4, 133.3, 131.4, 131.1, 131.0, 130.9, 130.4, 130.0, 129.6, 128.0, 127.9, 127.8, 127.7, 127.5, 127.4, 127.1, 126.8, 126.4, 125.9, 125.7 (aryl), 41.9 (d, J = 80 Hz, CH_2P); $^{31}P\{^1H\}$ NMR (CD_2Cl_2, 233 K) δ 38.74 (dt, J_{RhP} = 159 Hz, J_{PP} = 116 Hz, PPh_3), 34.94 (dt, J_{RhP} = 151 Hz, J_{PP} = 115 Hz), 32.25 (dt, J_{RhP} = 155 Hz, J_{PP} = 113 Hz); IR (CH_2Cl_2) 2012 (m), 1921 (s) cm^{-1}. Anal. Calcd for $C_{57}H_{48}OP_3Rh$: C, 72.46; H, 5.12. Found: C, 71.97; H, 5.06.

X-ray Crystal Structure Determination of 7·CH$_2$Cl$_2$. Crystals of (BISBI)Rh(PPh_3)(CO)H suitable for X-ray diffraction study were obtained by slow diffusion of hexane into a CH_2Cl_2 solution. 7·CH_2Cl_2 crystallized in the triclinic space group $P1$, a = 10.977 (3) Å, b = 14.469 (5) Å, c = 16.779 (6) Å, α = 101.29 (3)°, δ = 99.69 (3)°, γ = 106.33 (3)°, V = 2436.3 (14) Å^3. The structure was solved by direct methods, and remaining non-hydrogen atoms were located by a difference map. All non-hydrogen atoms were refined with anisotropic thermal parameters. Hydrogen atom locations (except the metal hydride) were calculated by using a riding model. The structure was refined to R = 0.035 and R_w = 0.039 for 5780 observed data. Crystal data and collection parameters, atomic coordinates, bond lengths, bond angles, anisotropic thermal parameters, H-atom coordinates, and a structure factor table are included in the supplementary material.

(BISBI)Rh(PPh$_3$)(^{13}CO)H (7-^{13}CO) was prepared by the reaction of $(Ph_3P)_3Rh(^{13}CO)H$ (14 mg, 0.015 mmol) and BISBI (9 mg, 0.016 mmol) in CD_2Cl_2. The ^1H NMR spectrum of the solution exhibited a hydride resonance at δ −10.43 (dtd, J_{CH} = 40, J_{PH} = 16, 6 Hz). The ^{13}C NMR spectrum exhibited a single resonance at δ 205.4 (tq, J_{CH} = J_{RhC} = 42 Hz, J_{PC} = 11 Hz, Rh–CO). Selective decoupling of the hydride signal at δ −10.43 resulted in the collapse of the resonance at δ 205.4 to a doublet of quartets with J_{RhC} = 42 Hz, J_{PC} = 16 Hz.

(BISBI)Rh(PPh$_3$)(CO)D (7-d). A solution of (BISBI)Rh(PPh_3)(CO)H (10 mg, 0.01 mmol) in 5 mL of CH_2Cl_2 was stirred for 1 h under 0.522 atm of D_2. The infrared spectrum of the solution exhibited a single band at 1974 (s) cm^{-1}.

(BISBI)Rh(CO)$_2$H (9). A solution of (BISBI)Rh(PPh_3)(CO)H (9 mg, 9 μmol) in CD_2Cl_2 was sealed under 0.70 atm of 1:1 CO/H_2. The solution was shaken and transferred to an NMR probe at −30 °C. The ^1H NMR spectrum of the solution exhibited a hydride resonance at δ −10.46 (td, J_{PH} = 16, 6 Hz), assigned to (BISBI)Rh(PPh_3)(CO)H, and a new hydride resonance at δ −10.77 (t, J_{PH} = 8 Hz) assigned to (BISBI)Rh$(CO)_2$H. Integration of the hydride resonances indicated a 1.2:1 ratio of 7:9: $^{31}P\{^1H\}$ NMR (CD_2Cl_2, −30 °C) δ 37.99 (dt, J_{RhP} = 159 Hz, J_{PP} = 115 Hz, PPh_3 of 7), 34.65 (dt, J_{RhP} = 151 Hz, J_{PP} = 114 Hz, BISBI P of 7), 32.06 (dt, J_{RhP} = 155 Hz, J_{PP} = 113 Hz, BISBI P of 7), 28.89 (d, J_{RhP} = 149 Hz, BISBI P of 9), −12.35 (s, free PPh_3).

(BISBI)Rh(^{13}CO)$_2$H (9-^{13}CO). A CD_2Cl_2 solution of BISBI and $(Ph_3P)_3Rh(^{13}CO)H$ was exposed to 0.611 atm of ^{13}CO at −10 °C. The ^1H NMR spectrum of the solution exhibited a hydride resonance at δ −10.46 (dtd, J_{CH} = 40 Hz, J_{PH} = 16 Hz, $J_{P'H}$ = 6 Hz), assigned to (BISBI)Rh(PPh_3)(^{13}CO)H, and a new hydride multiplet at δ −10.77 (tt, J_{CH} = 16 Hz, J_{PH} = 8 Hz) assigned to (BISBI)Rh(^{13}CO)$_2$H. Integration of the hydride resonances indicated a 1.2:1 ratio of 7-^{13}CO:9-^{13}CO. The $^{13}C\{^1H\}$ NMR spectrum exhibited a resonance at δ 205.0 (dq, J_{RhC} = 43 Hz, J_{PC} = 12 Hz) assigned to the carbonyl resonance of (BISBI)Rh(PPh_3)(^{13}CO)H. A multiplet at δ 199.3 (dt, J_{RhC} = 61 Hz, J_{PC} = 10 Hz) is assigned to (BISBI)Rh(^{13}CO)$_2$H.

Low-Temperature Infrared Spectrum of (BISBI)Rh(CO)$_2$D (9-d). A solution of (BISBI)Rh(PPh_3)(CO)H (35 mg, 0.037 mmol) in 20 mL of CH_2Cl_2 was stirred under 1 atm of D_2 for 1 h. The infrared spectrum of the solution at −78 °C exhibited a single band at 1969 cm^{-1} assigned to (BISBI)Rh(PPh_3)(CO)D (9-d). Carbon monoxide was then bubbled through the solution at −78 °C for 1.5 h. The solution was syringed into a low-temperature infrared cell which had been purged with carbon monoxide. The IR spectrum of the solution at −78 °C exhibited two bands of equal intensity at 2017 and 1958 cm^{-1}.

(BISBI)Ir(PPh$_3$)(CO)H (10). A solution of $(PPh_3)_3Ir(CO)H$ (120 mg, 0.119 mmol) and BISBI (66 mg, 0.120 mmol) in 10 mL of CH_2Cl_2 was stirred at 25 °C for 4 h. Solvent was evaporated under vacuum. The resulting solid was stirred in 10 mL of methanol for 30 min and filtered to yield (BISBI)Ir(PPh_3)(CO)H (**10**) (133 mg, 84% yield) as a bright yellow powder: ^1H NMR δ 7.8–5.9 (m, aromatic), 4.9–3.6 (m, CH_2P), −11.51 (td, J_{PH} = 24, $J_{P'H}$ = 15 Hz, IrH); $^{13}C\{^1H\}$ NMR (CD_2Cl_2) δ 187.2 (broad s, IrCO), 140.5 (d, J = 37 Hz), 138.2, 136.7 (d, J = 14 Hz), 136.2 (d, J = 15 Hz), 135.0, 133.3 (d, J = 12 Hz), 131.3, 131.1, 131.0, 130.3, 130.1, 129.9, 129.3, 129.2, 128.6, 128.2, 127.7, 127.6 (d, J = 26 Hz), 127.1, 127.0, 126.4, 125.9, 125.7 (biphenyl and phenyl), 44.3 (virtual triplet, peak separation = 13 Hz, CH_2P), 43.0 (virtual triplet, peak separation = 15 Hz, CH_2P); $^{31}P\{^1H\}$ NMR (CD_2Cl_2) δ 14.44, 13.76, 9.76 (ABX, J_{PA-PB} = 122 Hz, J_{PA-PX} = 140 Hz, J_{PB-PX} = 122 Hz); IR (CH_2Cl_2) 2075 (m), 1932 (s) cm^{-1}. Analytically pure material was obtained by recrystallization from hexane and a small amount of CH_2Cl_2. Anal. Calcd for $C_{57}H_{48}IrOP_3$: C, 66.20; H, 4.68. Found: C, 65.86; H, 4.81.

(BISBI)Ir(CO)$_2$H (11). A solution of (BISBI)Ir(PPh_3)(CO)H (**10**) (400 mg, 0.386 mmol) in 25 mL of toluene was stirred under 1 atm of CO at 25 °C, and 45 mL of a CO-saturated solution of ethanol was added. The solid which crystallized from solution overnight was filtered, washed with toluene/ethanol, and dried under vacuum to give **11** (225 mg, 73% yield) as a pale yellow powder: ^1H NMR (200 MHz, CD_2Cl_2) δ 7.6–6.2 (m, aromatic), 4.05 (m, CH_2P), −12.12 (t, J_{PH} = 16 Hz, 1 H, IrH); $^{13}C\{^1H\}$ (CD_2Cl_2) δ 183.6 (t, J_{PC} = 15 Hz, IrCO), 144.37 (virtual t, J = 23 Hz), 142.3, 137.5 (virtual t, J = 22 Hz), 135.6, 135.4 (t, J = 8 Hz), 131.2, 130.8, 130.6, 130.4, 128.8, 128.2, 128.0, 127.7, 127.1, 126.4 (biphenyl and phenyl), 29.9 (AA'XX', J_{PC} = 19 Hz, $J_{PP} \approx$ 300 Hz, CH_2P); $^{31}P\{^1H\}$ (CD_2Cl_2) δ 4.3 (s); IR (CH_2Cl_2) 2074 (w), 1985 (s), 1932 (s) cm^{-1}.

X-ray Crystal Structure Determination of 11·$^1/_2$O(CHMe$_2$)$_2$. Crystals of (BISBI)Ir$(CO)_2$H suitable for X-ray diffraction study were obtained by slow evaporation of a solution of **11** in 1:1 $CH_2Cl_2/O(CHMe_2)_2$ under a CO atmosphere. Pale yellow transparent crystals turned white and opaque at room temperature in air. This decomposition may be the result of CO or solvent loss. After several unsuccessful attempts to collect room-temperature X-ray data, low-temperature X-ray data was obtained by mounting a crystal on the tip of a thin glass fiber and quickly placing the crystal under a cold nitrogen stream. No decomposition of the crystal was observed during data collection. Four molecules of **11** and two $O(CHMe_2)_2$ molecules crystallized in a monoclinic unit cell, with space group symmetry $P2_1/c$, a = 10.842 (8) Å, b = 17.17 (2) Å, c = 19.08 (1) Å, β = 95.76 (6)°, and V = 3534 (6) Å^3. The iridium position was determined by direct methods, and the remaining non-hydrogen atoms were located by successive Fourier difference maps. All non-hydrogen atoms were refined with anisotropic thermal parameters. All hydrogen atoms (except the metal hydride) were fixed at idealized positions and with isotropic thermal parameters fixed at U = 0.08 Å^2. Difference maps also disclosed six independent residual peaks near a center of symmetry at 0,0,0; these peaks were interpreted as two symmetry-related $O(CHMe_2)_2$ molecules per unit cell possessing a centrosymmetric crystal disorder with each solvent molecule distributed between two orientations related by an average center of symmetry. Five of the six peaks, which were assigned to the isopropyl methyl carbons and to the oxygen, were given half-weighted occupancy. The structure was refined to R = 0.062 and R_w = 0.071 for 4169 observed data. Crystal data and collection parameters, atomic coordinates, bond lengths, bond angles, anisotropic thermal parameters, H-atom coordinates, and a structure factor table are included in the supplementary material.

[T-BDCP]Rh[P(C$_6$H$_4$-*p*-CH$_3$)$_3$](CO)H (12). A solution of *trans*-1,2-bis[(diphenylphosphino)methyl]cyclopropane (T-BDCP, **2**) (136 mg, 0.310 mmol) and Rh[P(C_6H_4-*p*-CH_3)$_3$]$_3$(CO)H[13] (311 mg, 0.288 mmol) was stirred in 5 mL of CH_2Cl_2 for 6 h. Solvent was evaporated under vacuum, 10 mL of Et_2O was added, and the solution was filtered. Evaporation of Et_2O under vacuum gave 303 mg of a mixture of **12** and P(C_6H_4-*p*-CH_3)$_3$ as a bright yellow solid. ^1H and ^{31}P integration indicated ~2 mol of P(C_6H_4-*p*-CH_3)$_3$ per mole of **12**. Attempts to separate **12** and P(C_6H_4-*p*-CH_3)$_3$ by recrystallization and chromatography were unsuccessful: ^1H NMR (CD_2Cl_2) δ 7.5–6.8 (m, aromatic), 2.34 (s, CH_3 of free P(C_6H_4-*p*-CH_3)$_3$), 2.27 (s, CH_3 of **12**), −10.42 (q, J_{PH} = 16 Hz, RhH); $^{31}P\{^1H\}$ NMR (CD_2Cl_2) ABCRh pattern δ 38.2, 37.5, 36.8 (J_{PA-Rh} = 152 Hz, J_{PA-PB} = 123 Hz, J_{PA-PC} = 123 Hz, J_{PB-Rh} = 155 Hz, J_{PB-PC} = 123 Hz, J_{PC-Rh} = 152 Hz), −7.5 (s, P(C_6H_4-*p*-CH_3)$_3$; IR (CH_2Cl_2) 1989 (s), 1908 (w) cm^{-1}.

(28) Varshavskii, Y. S.; Cherkasova, T. G. *Russ. J. Inorg. Chem.* **1967**, *12*, 899.
(29) Yagupsky, M.; Wilkinson, G. *J. Chem. Soc. A* **1970**, 941.
(30) Ahmad, N.; Levison, J. J.; Robinson, S. D.; Uttley, M. F. *Inorg. Synth.* **1974**, *15*, 59.

The deuteride **12**-d was prepared from a CH_2Cl_2 solution of **12** under 1 atm of D_2: IR (CH_2Cl_2) 1955 cm^{-1}.

(T-BDCP)Rh(CO)$_2$H (14). A solution of **12** (6 mg, 1:2 mixture of **12**/$P(C_6H_4$-p-$CH_3)_3$) in CD_2Cl_2 was prepared under 0.56 atm of 1:1 CO/H_2 and immediately placed in an NMR probe at 258 K. The ^1H NMR spectrum of the solution exhibited a multiplet at δ −10.50 (q, J_{PH} = 16 Hz) due to **12** and a multiplet at δ −9.87 (td, J_{PH} = 16 Hz, J_{RhH} = 6 Hz) assigned to the dicarbonyl hydride **14**. Integration of the hydride resonances indicated a 1.6:1 ratio of **12** and **14**. The $^{31}P\{^1H\}$ NMR spectrum exhibited an ABCRh pattern centered at δ 37.5 due to compound **12** and a doublet at δ 32.3 (d, J_{RhP} = 130 Hz) assigned to **14**. A singlet due to free $P(C_6H_4$-p-$CH_3)_3$ was observed at δ −7.5.

Catalytic Hydroformylation of 1-Hexene. Hydroformylation reactions were performed in a 90-mL Fischer–Porter bottle equipped with a gas inlet valve, liquid sampling valve, and star-head magnetic stir bar. The pressure apparatus was immersed in a constant-temperature bath maintained at 33.6 ± 0.5 °C in a well-ventilated fume hood. A magnetic stirrer placed below the bath provided efficient stirring.

(acac)Rh(CO)$_2$[25] (7.9 mg, 0.031 mmol) and a chelating diphosphine (0.031 mmol) were placed in the pressure apparatus under nitrogen. The system was flushed with 70 psig of CO/H_2 three times and then pressurized to 70 psig with analyzed CO/H_2 (50.02% CO, 49.98% H_2). Benzene (6.0 mL) and toluene (internal GC standard, 0.20 mL, 1.9 mmol) were added by gastight syringe to the pressurized system. After 1 h of stirring, 1-hexene (2.50 mL, 0.020 mmol) was added. The pressure of the system was maintained throughout the reaction by adding additional CO/H_2 periodically. Samples were removed via the liquid sampling valve for analysis. Heptanal and 2-methylhexanal were analyzed by temperature-programmed gas chromatography on an HP5890A chromatograph interfaced to a HP3390A integrator using a 10 m × 0.53 mm methyl silicone capillary column.

Acknowledgment. Financial support from the Department of Energy, Division of Basic Energy Sciences, is gratefully acknowledged. L.M.P. thanks the National Science Foundation for a predoctoral fellowship. We thank Texas Eastman for a generous gift of BISBI and Johnson-Matthey for a loan of rhodium salts.

Registry No. 1, 141434-93-7; (±)-**2**, 141434-94-8; **3**, 125282-09-9; **4**, 17185-29-4; **7**, 141376-55-8; **7**·CH_2Cl_2, 141396-43-2; **7**-^{13}CO, 141376-64-9; **7**-*d*, 141376-60-5; **9**-ea, 141376-56-9; **9**-ea-^{13}CO, 141376-63-8; **9**-ea-*d*, 141376-61-6; **10**, 141376-57-0; **11**, 141376-58-1; **11**·$^1/_2$O-$(CHMe_2)_2$, 141376-62-7; **12**, 141396-44-3; **12**-*d*, 141396-45-4; **14**, 141376-59-2; (+)-DIOP, 37002-48-5; DIPHOS, 1663-45-2; $(Ph_3P)_3$Rh-(CO)H, 17185-29-4; $(Ph_3P)_3$Rh(^{13}CO)H, 141376-65-0; $(Ph_3P)_3$Ir-(CO)H, 33541-67-2; Rh[$P(C_6H_4$-p-$CH_3)_3]_3$(CO)H, 27709-98-4; (acac)Rh(CO)$_2$, 14874-82-9; 1-hexene, 592-41-6.

Supplementary Material Available: Tables of crystal data and collection parameters, atomic coordinates, bond lengths, bond angles, thermal parameters, and H-atom coordinates (19 pages); listings of observed and calculated structure factors for (BISBI)Rh(PPh_3)(CO)H·CH_2Cl_2 (**7**·CH_2Cl_2) and (BISBI)Ir(CO)$_2$H (**11**·$^1/_2$O$(CHMe_2)_2$) (38 pages). Ordering information is given on any current masthead page.

A Receptor-Mediated Immune Response Using Synthetic Glycoconjugates

Carolyn R. Bertozzi and Mark D. Bednarski*

Contribution from the Department of Chemistry, University of California, Berkeley, California 94720. *Received January 21, 1992*

Abstract: Antibody recognition of bacterial pathogens is important for activating complement and macrophage-mediated processes. Many bacterial antigens, however, undergo genetic variation to avoid antibody recognition. A synthetic glycoconjugate can direct antibodies to *E. coli* cells via their type 1 pili mannose-specific receptors. The receptor targeted antibodies activate both complement and macrophage-mediated processes that result in cell death. Bacterial cell-surface receptors can therefore be exploited to confer antigenicity onto the organism.

Introduction

Antibody-mediated pathways in humoral and cellular immunity include complement activation and receptor-mediated phagocytosis.[1–4] These processes rely upon the coating of the pathogen with antibodies and recognition of the Fc region of the antibodies by effector molecules such as complement factor C1q and macrophage Fc receptors.[5,6] Several strains of enterobacteria express proteinaceous appendages called pili that present antigenic recognition sites for the host's immune system.[4,7] Type 1 pili also contain receptors specific for terminal α-linked mannosides which mediate the adhesion of bacteria to host cells, a process that is essential for infectivity.[8–14] We report herein that antibodies directed to the bacterial cells by a synthetic mannosyl glycoconjugate activate both complement and macrophage-mediated processes that result in cell killing. The conserved binding domain of cell-surface receptors can therefore be utilized to direct antibodies to pathogens and prime them for killing by host defense mechanisms.

Early work toward the introduction of antigenic components onto otherwise non-immunogenic cells focused on the covalent modification of target cells in vitro with immunogenic small molecules such as trinitrophenol (TNP).[15,16] These covalently altered model systems were particularly useful for studying the

(1) Joiner, K. A.; Brown, E. J.; Frank, M. M. *Annu. Rev. Immunol.* **1984**, *2*, 461.
(2) Soderstrom, T.; Ohman, L. *Scand. J. Immunol.* **1984**, *20*, 299.
(3) Ofek, I.; Sharon, N. *Infect. Immun.* **1988**, *56*, 539.
(4) Virji, M.; Heckels, J. E. *Infect. Immun.* **1985**, *49*, 621.
(5) Reid, K. B. M.; Porter, R. R. *Annu. Rev. Biochem.* **1981**, *50*, 433.
(6) (a) Silverstein, S. C.; Steinman, R. M.; Cohn, Z. A. *Annu. Rev. Biochem.* **1977**, *46*, 669. (b) Duncan, A. R.; Woof, J. M.; Partridge, L. J.; Burton, D. R.; Winter, G. *Nature* **1988**, *332*, 563.
(7) Clegg, S.; Gerlach, G. F. *J. Bacteriol.* **1987**, *169*, 934.
(8) Firon, N.; Ofek, I.; Sharon, N. *Infect. Immun.* **1984**, *43*, 1088.
(9) Firon, N.; Ofek, I.; Sharon, N. *Carbohydr. Res.* **1983**, *120*, 235.
(10) Ofek, I.; Mirelman, D.; Sharon, N. *Nature* **1977**, *265*, 623.
(11) Eshdat, Y.; Ofek, I.; Yashouv-Gan, Y.; Sharon, N.; Mirelman, D. *Biochem. Biophys. Res. Commun.* **1978**, *85*, 1551.
(12) Hanson, M. S.; Brinton, C. C., Jr. *Nature* **1988**, *332*, 265.
(13) Hanson, M. S.; Hempel, J.; Brinton, C. C., Jr. *J. Bacteriol.* **1988**, *170*, 3350.
(14) Bloch, C. A.; Orndorff, P. E. *Infect. Immun.* **1990**, *58*, 275.
(15) Shearer, G. M.; Rehn, T. G.; Garbarino, C. A. *J. Exp. Med.* **1975**, *141*, 1348.
(16) Henkart, P. A.; Schmitt-Verhulst, A.-M.; Shearer, G. M. *J. Exp. Med.* **1977**, *146*, 1068.

0002-7863/92/1514-5543$03.00/0